

Supporting Information

Mixed-metal Zr/Ti MIL-173 porphyrinic metal-organic frameworks as efficient photocatalysts towards solar-driven overall water splitting

Ben Gikonyo,^a Eva Montero Lanzuela,^b Herme G. Boldovi,^b Siddhartha De,^a Catherine Journet,^a Thomas Devic,^c Nathalie Guillou,^d Davide Tiana,^e Sergio Navalon^b and Alexandra Fateeva^a

^a*Laboratoire des Multimatériaux et Interfaces, Université Lyon, Université Claude Bernard Lyon 1, UMR CNRS 5615, F-69622 Villeurbanne, France*

^b*Departamento de Química, Universitat Politècnica de València, C/Camino de Vera, s/n, 46022 Valencia, Spain*

^c*Institut des Matériaux Jean Rouxel, Université de Nantes, UMR CNRS 6502, 44322 Nantes, France*

^d*Institut Lavoisier de Versailles, UMR 8180 CNRS UVSQ, Université Paris-Saclay, 45 avenue des Etats-Unis, 78035 Versailles, France*

^e*School of Chemistry, University College Cork, College Rd, Cork, Ireland*

Table of contents

| | |
|--|-------|
| A. Materials and methods..... | SI-3 |
| ◆ X-Ray Diffraction | SI-3 |
| ◆ Electronic microscopy | SI-3 |
| ◆ Adsorption measurements | SI-3 |
| ◆ Thermogravimetric analysis (TGA) | SI-3 |
| ◆ X-ray photoelectron spectroscopy | SI-4 |
| ◆ Photocatalytic experiments | SI-4 |
| ◆ Photophysical measurements..... | SI-4 |
| B. Computational Details | SI-6 |
| C. Synthetic procedures | SI-8 |
| ◆ MIL-173(Zr) synthesis..... | SI-8 |
| ◆ Post-synthesis Metal Exchange of MIL-173(Zr) | SI-8 |
| ◆ In-situ synthesis of mixed metal MIL-173(Ti/Zr)..... | SI-8 |
| D. Characterizations of the samples obtained by post-synthesis metal exchange | SI-9 |
| E. Characterizations of the samples obtained by one-pot synthesis using Ti isopropoxide..... | SI-10 |
| F. Characterizations of the samples obtained <i>in-situ</i> using TiBALD..... | SI-12 |
| G. Characterizations of the samples after photocatalysis | SI-21 |
| References | SI-22 |

A. Materials and methods

All chemicals were purchased from commercial sources and used without any further purification. 5,10,15,20-tetrakis(3,4,5-trihydroxyphenyl)porphyrin (H₁₄TGalPP) has been prepared according to the reported procedure¹.

◆ *X-Ray Diffraction*

Powder X-Ray diffraction (PXRD) was performed on a PANalytical XpertPro MRD diffractometer with a Cu K α 1 radiation ($\lambda = 1.540598 \text{ \AA}$) used with 40 kV and 30mA settings in θ/θ mode, reflection geometry.

High resolution Powder X-Ray diffraction was recorded at room temperature on a Bruker D8 Advance diffractometer with a Debye-Scherrer geometry, in the 2θ range 4-90°. The D8 system is equipped with a Ge(111) monochromator producing Cu K α 1 radiation ($\lambda = 1.540598 \text{ \AA}$) and a LynxEye detector.

◆ *Electronic microscopy*

Scanning Electron Microscopy images were recorded on FEI Quanta 250 FEG microscope.

The Energy Dispersive Spectroscopy analysis was performed by scanning electron microscopy on FEI Quanta 250 FEG and Zeiss Merlin Compact microscopes in the microscopy center of Lyon1 University. Samples were mounted on stainless pads and sputtered with $\sim 2 \text{ nm}$ of carbon to prevent charging during observation.

Transmission Electron Microscopy was performed on JEOL 2100F microscope operating at 200 kV and equipped with an 80 mm² Oxford EDS analysis detector. Each of the samples was prepared by ultrasonication in ethanol and deposited on a TEM copper grid (300 mesh) covered with a holey carbon support film.

◆ *Adsorption measurements*

Surface areas were measured by N₂ adsorption and desorption at 77.3 K using a BEL Japan Belsorp Mini apparatus volumetric adsorption analyzer. The sample was pre-activated under vacuum at 130°C prior to sorption measurement. The BET surface calculations were performed using points at the pressure range $0 < P/P^\circ < 0.15$.

◆ *Thermogravimetric analysis (TGA)*

TGA was performed with a TGA/DSC 1 STAR^e System from MettlerToledo. Around 5-10 mg of sample is heated at a rate of 10 K·min⁻¹ from 25 to 800 °C, in a 70 μL alumina crucible, under air atmosphere (20 mL·min⁻¹).

◆ X-ray photoelectron spectroscopy

X-ray photoelectron spectroscopy (XPS) analyses for the MIL-173(Zr) and MIL-173(Zr/Ti)-40 solids were recorded using a SPECS spectrometer equipped with a multichannel (MCD-9) detector and using a monochromatic Al ($K\alpha=1486.6$ eV) X-ray source. CasaXPS processing software was employed for spectra deconvolution using the C 1s peak at 284.4 eV as binding energy reference.

◆ Photocatalytic experiments

The photocatalytic overall water splitting experiments were carried out at least in triplicate. Briefly, a quartz reactor (51 mL) containing the required amount of MOF (ca 10 mg) in Milli-Q water (20 mL) was sonicated for 30 min (450 W powder) and, then, the system purged with argon for 1 h. Simulated solar light irradiation were performed using a commercially available Hamamatsu spot light source (150 W Hg-Xe lamp ref L8253; spot light source L9566-04; light guide A10014-50-0110) equipped with a AM 1.5 G filter (Lasing, ref. 81094). Visible light irradiations were carried out using commercially available filters namely GG420 (Microbeam; > 420 nm) and GG495 (Thorlabs, > 495 nm). A commercially available visible band pass filter at 450 nm (Thorlabs, FB450-10) was employed to estimate the apparent quantum yield (AQY). As previously reported,² the AQY defined as the number of reacted electrons respect to the number of incident photons can be estimated using the following equation:

$$AQY (\%) = \frac{\text{Number of reacted electrons}}{\text{Number of incident photons}} \times 100$$

$$AQY (\%) = \frac{2 \cdot \text{Number of hydrogen molecules evolved}}{\text{Number of incident photons}} \times 100 = \frac{2 \cdot n_{H_2,t} \cdot N_A \cdot h \cdot c}{P \cdot S \cdot \lambda_{inc} \cdot t} \times 100$$

where $n_{H_2,t}$ is the number H_2 moles evolved during the duration (t) of the incident light exposure, N_A is the Avogadro's constant, h (J·s) is Planck's constant, c ($m \cdot s^{-1}$) is the speed of light, P ($W \cdot m^{-2}$) is the power density of the incident monochromatic light, S (m^2) is the irradiation area, λ_{inc} (m) is the wavelength of the incident monochromatic light and t (s) is the duration of the incident light exposure.

The evolved H_2 and O_2 gases were analyzed from the headspace gas using an Agilent 490 Micro GC system equipped with a molecular sieve column (5 Å) and using argon as carrier gas. The temperature and the pressure of the reactor were monitored by means of a thermometer and a manometer, respectively.

◆ Photophysical measurements

Solid state UV-vis spectroscopy was performed with Perkin Elmer Lambda 365 Spectrophotometer at room temperature using an integrating sphere. MOF samples were diluted in KBr so the absorption maximum signal remained lower than 0.6.

Photocurrent measurements were carried out in a traditional electrochemical cell with three electrodes. The working electrode consisted in a transparent fluoride-doped tin oxide (FTO)-coated glass substrate where a thin layer of MIL-173(Zr) or MIL-173(Zr/Ti)-40 solids were deposited. A platinum wire and a standard calomel electrode were employed as counter and reference electrodes, respectively. The system containing acetonitrile as solvent and tetrabutylammonium hexafluorophosphate (TBAPF₆) as electrolyte was purged with an argon stream for 30 min. The current was measured under both dark and illumination conditions (150 W He-Xe lamp) after polarizing the working electrode at potentials from 0.2 to 1.4 V. Analogous photocurrent experiments were also carried out in the presence of methanol (0.3 mL) as sacrificial electron donor.

Photoluminescence measurements were performed with a FLS1000 spectrofluorometer (Edinburgh Instruments, Livingston, UK), equipped with an N-DMM double-emission monochromator, an N-G11 PMT-980 detector, and equipped with a pulsed Xe lamp (450W) as the excitation source. Samples were measured with a quartz cuvette of 4 mL with optical length of 1 cm x 1 cm. Before measuring, samples in acetonitrile were prepared after sonicating and purging with argon for 10 min, then its absorbance was adjusted to 0.4 (a.u.) at the excitation wavelength (440 nm).

B. Computational Details

A standard procedure adopted in previous publications were used. The geometry and the electronic structure were optimized using the quantum espresso program³. All the geometry optimizations were performed at the gamma point using the semi-local PBEsol⁴ exchange correlation functional, using norm-conserving pseudopotentials with a cut-off of 90 Ry. A reduced cell with symmetry p1 was created starting from the experimental structure. The reduced cell contains 312 atoms (8 Zr, 16 N, 54 O, 176 C, 64 H) and this lattice parameters: $a = 14.99 \text{ \AA}$, $b = c = 21.465 \text{ \AA}$; $\alpha = 82.99^\circ$, $\beta = \gamma = 69.55^\circ$. Both the atomic positions and the lattice parameters were relaxed during the optimization. The force and energy thresholds were set to $1\text{E-}05 \text{ Ry}$ and $1\text{E-}04 \text{ Ry}$, respectively, while the pressure convergence was set to $1\text{E-}01 \text{ Kbar}$. The optimization with an SCF convergence threshold was set to $1\text{E-}06$. After having optimized the pristine Zr-MOF, Zr atoms were then replaced with Ti in the following ratios: 1/8; 2/8; 3/8; 4/8, corresponding to 12.5, 25, 37.5 and 50 Ti atomic % respectively. For the 2/8, 3/8 and 4/8 systems, different configurations of Ti atoms were tested.

Tables S1-3 show difference in energy between the different configurations. The most stable configuration for each system (-54512.58 eV for 2/8, -54515.78 eV for 3/8 and -54520.24 eV) has been set for reference as 0.

Table S1. energy differences for different configuration for 25 at% Ti in MIL-173(Zr/Ti)-25.

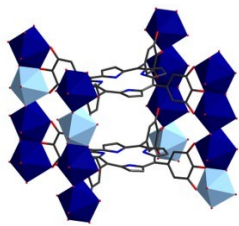
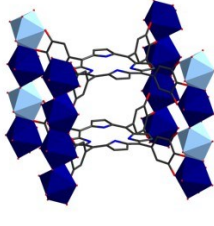
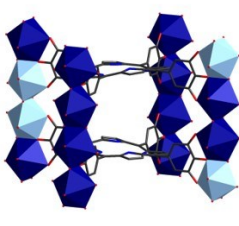
| configuration 1 0 eV | configuration 2 0.11 eV | configuration 3 0.18 eV |
|---|---|--|
|  |  |  |

Table S2. energy differences for different configuration for 37.5 at% Ti in MIL-173(Zr/Ti)-37.5.

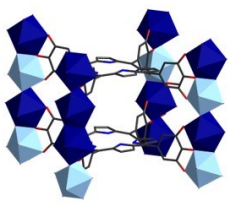
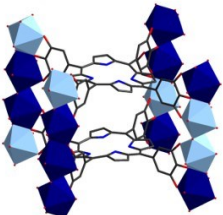
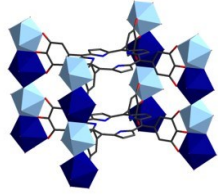
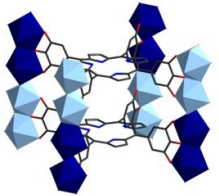
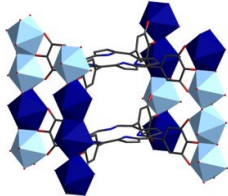
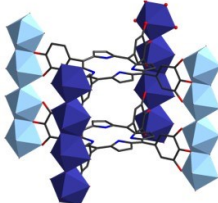
| configuration 1 0 eV | configuration 2 0.11 eV |
|---|---|
|  |  |

Table S3. energy differences for different configuration for 50 at% Ti in MIL-173(Zr/Ti)-50.

| configuration 1 0 eV | configuration 2 0.21 eV | configuration 3 0.32 eV | configuration 4 0.68 eV |
|---|---|--|---|
|  |  |  |  |

For each system: pristine Zr, 12.5%, 25%, 37.5% and 50% the most stable optimized configuration was used to analyze the frontier orbitals and the theoretical internal surface.

The frontier orbitals and the band gap were then calculated by performing single point calculations at the PBEsol optimized geometries using the non-local hybrid GAUPBE functional⁵.

The theoretical surface and accessible volume were calculated using the code Zeo++, which is the standard code used for calculating accessible internal surfaces and volumes of porous materials^{6,7}. After having performed a Voronoi decomposition of the space, the accessible internal surface and volume are calculated with a Monte Carlo simulation using a probe of radius r to simulate the guest molecule inside of the pore. Despite producing good result, it should be noted that the following limitations are present for this approximation: (1) the guest molecule is assumed to be a perfect sphere, which is not the case of N_2 ; (2) the simulations are static, i.e., vibration due to thermal motions and crystal structure changes upon adsorption (e.g., pore swelling or ligand rotation) are not considered. As demonstrated by Ongari *et al.*, this can lead to discrepancy when dealing with narrow channels or small pores.

C. Synthetic procedures

◆ MIL-173(Zr) synthesis

MIL-173(Zr) was synthesized according to the reported procedure but with some modifications⁸. H₁₄TGalPP (100 mg, 0.12mmol) was combined with 5.6 mL of DMF and 3.2 mL of 1M HCl aqueous solution in a 40 mL glass vial. The resultant mixture was sonicated for 5 minutes to dissolve the ligand. Then, 1.2 mL of a freshly prepared 0.133M solution of ZrCl₄ (0.16 mmol) in 1M aqueous HCl was added and again sonicated for 10 minutes at room temperature. The mixture was heated at 130 °C for 23 hours using 3 hours heating and cooling ramps. The solid was recovered by centrifugation, washed 4 times with DMF and 3 times with methanol. The recovered solid was then soaked for 12 hours in methanol and washed once with methanol before drying overnight in the Schlenk line at 150 °C.

◆ Post-synthesis Metal Exchange of MIL-173(Zr)

50 mg of activated MIL-173(Zr) was inserted in a Schlenck tube and placed under vacuum at 100°C for 4 hours to remove any traces of water. Anhydrous DMF (5 mL) was added under inert atmosphere, followed by the addition of Ti-isopropoxide solution (tests with 0.5 and 1 eq of titanium were performed). The suspension was left to react for 48 hours. The solids were then collected by centrifugation and washed three times with DMF and three times with methanol.

◆ In-situ synthesis of mixed metal MIL-173(Ti/Zr)

With Ti isopropoxide

10% Ti-doped MIL-173(Zr) was synthesized by combining H₁₄TGalPP (100 mg, 0.12mmol), 5.6 mL of DMF, and 3.2 mL of 1M HCl aqueous solution in a 40 mL glass vial. The resultant mixture was sonicated for 5 minutes to dissolve the ligand. Then, 1.17 mL of a freshly prepared 0.133M solution of ZrCl₄ (0.151 mmol) in 1M aqueous HCl was added followed by 0.124 mL of 0.133M solution of titanium isopropoxide (0.016 mmol) in 1M aqueous HCl. The mixture was again sonicated at room temperature for 10 minutes and then heated at 130 °C for 23 hours using 3 hours heating and cooling ramps. MIL-173 (Ti/Zr) with different Ti percentages was achieved by only varying the Ti and Zr ratios in the reaction solution. The resultant solids were recovered like in case of MIL-173(Zr).

With TiBALD

10% Ti-doped MIL-173(Zr) was synthesized by combining H₁₄TGalPP (100 mg, 0.12mmol), 5.6 mL of DMF, and 3.2 mL of 1M HCl aqueous solution in a 40 mL glass vial. The resultant mixture was sonicated for 5 minutes to dissolve the ligand. Then, 1.17 mL of a freshly prepared 0.133M solution of ZrCl₄ (0.151 mmol) in 1M aqueous HCl was added followed by 8.4 μL of TiBALD (50% weight in water solution). The mixture was again sonicated at room temperature for 10 minutes and then heated at 130 °C for 23 hours using 3 hours heating and cooling ramp. MIL-173 (Ti/Zr) with different Ti percentages was also achieved by varying the Ti and Zr ratios in the reaction solution. The resultant solids were recovered with the same procedure as MIL-173(Zr).

D. Characterizations of the samples obtained by post-synthesis metal exchange

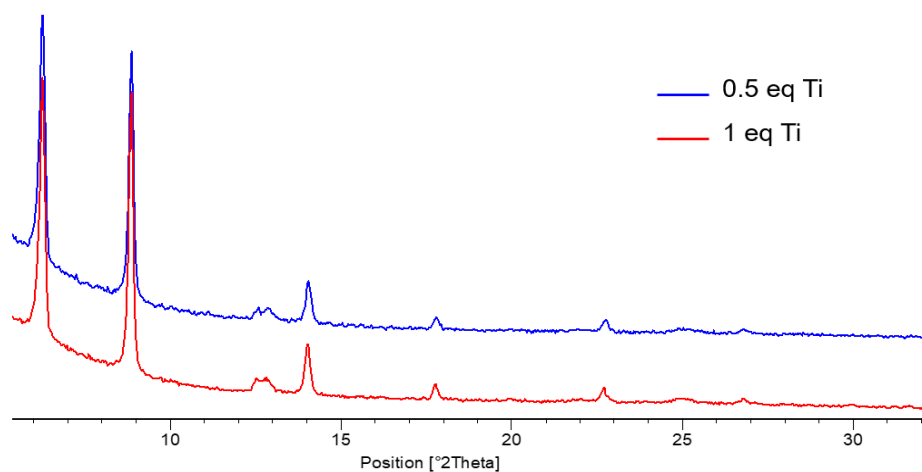


Figure S1: PXRD patterns for the solids obtained after PSME using 0.5 and 1 eq of titanium precursor.

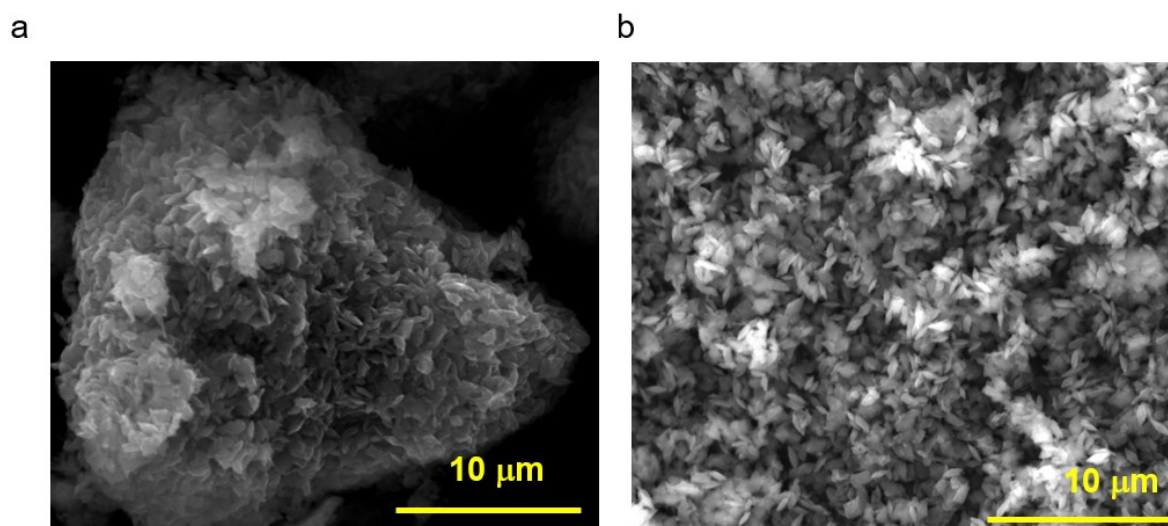


Figure S2: SEM images of the solids obtained by PSME with 1 eq of titanium (a) and 0.5 eq of titanium (b).

Table S4: Average Ti/Zr ratios obtained from EDS data (9 points analysis).

| SAMPLE | AVERAGE Ti/Zr | STANDARD DEVIATION |
|-------------------|---------------|--------------------|
| 1 eq Ti by PSME | 0.99 | 0.71 |
| 0.5 eq Ti by PSME | 0.85 | 0.46 |

E. Characterizations of the samples obtained by one-pot synthesis using Ti isopropoxide

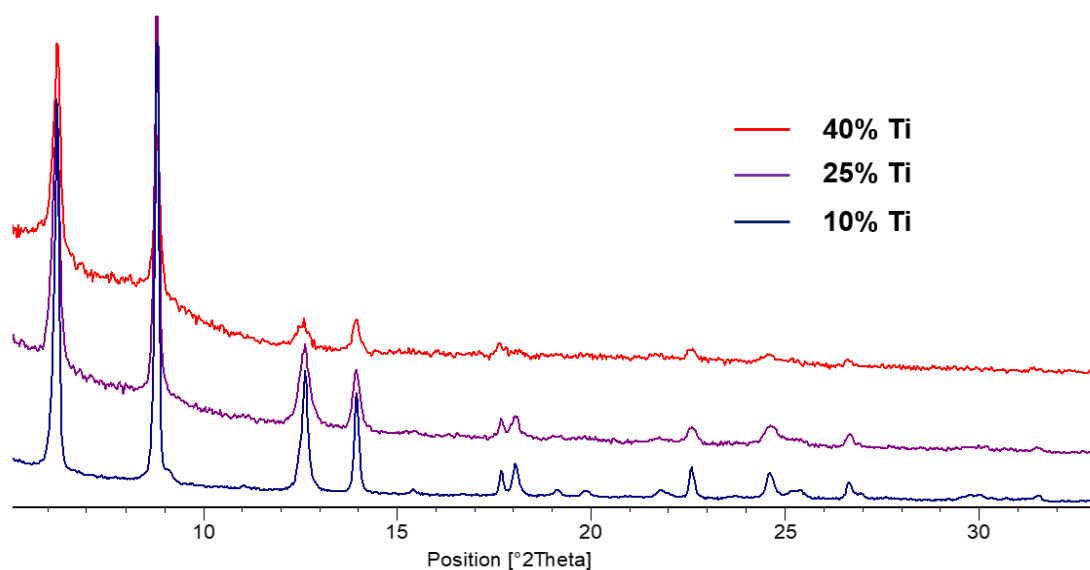


Figure S3: PXRD patterns of the solids obtained in-situ with titanium isopropoxide and zirconium chloride precursors, at variable titanium contents in the reaction solution.

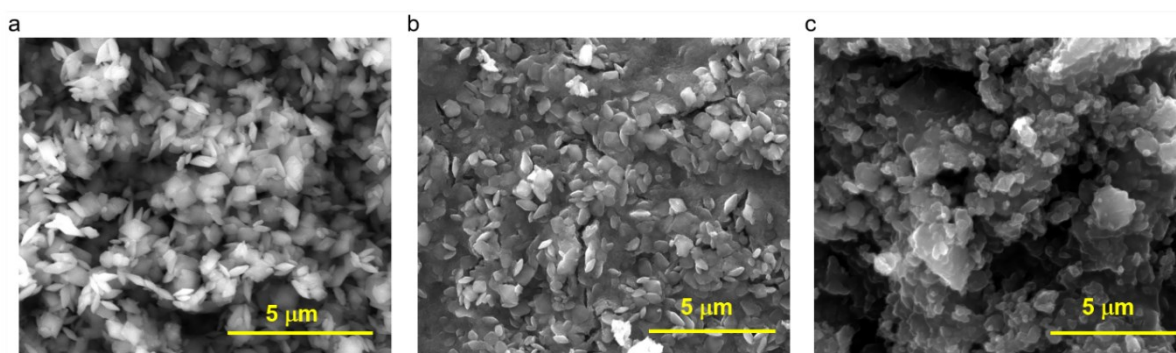


Figure S4: SEM images of the solids obtained by one-pot strategy with titanium isopropoxide and zirconium chloride precursors for 10% titanium (a), 25% titanium (b), and 40% titanium (c) in the reaction solution.

Table S5: EDS data (9 points analysis) for samples obtained using titanium isopropoxide.

| SAMPLE | THEOR Ti/Zr | AVERAGE Ti/Zr | STANDARD DEVIATION |
|--------|-------------|---------------|--------------------|
| 10% Ti | 0.11 | 0.13 | 0.01 |
| 25% Ti | 0.33 | 0.37 | 0.03 |
| 40% Ti | 0.67 | 0.70 | 0.05 |

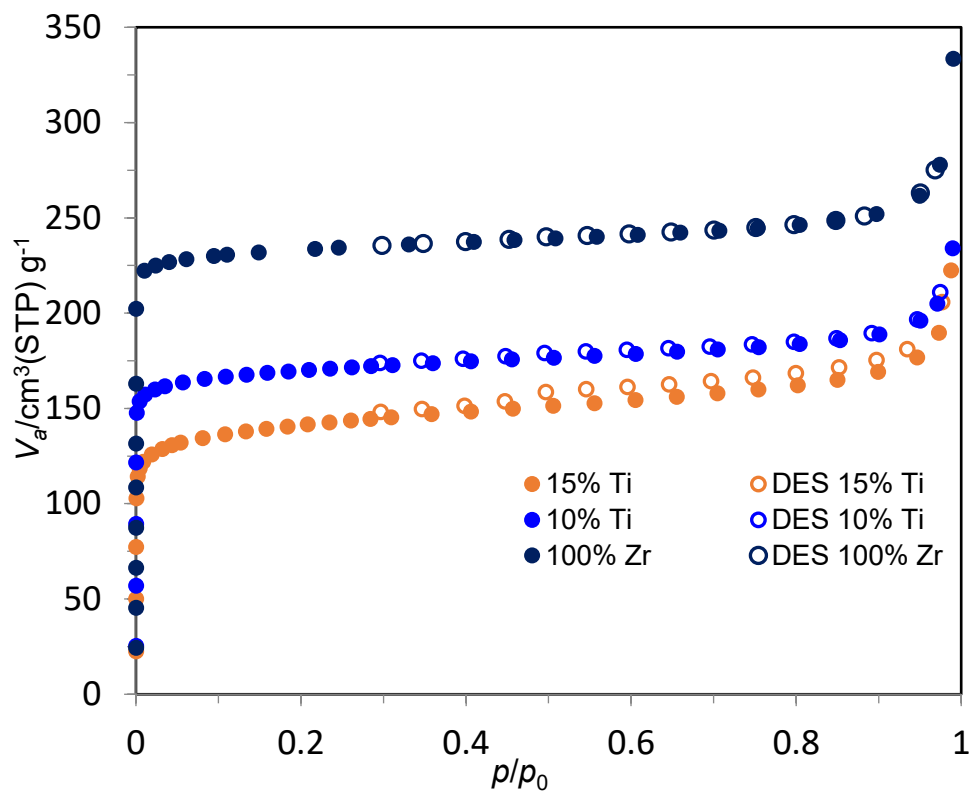


Figure S5: Nitrogen sorption isotherms at 77K for samples synthesized in-situ using Ti-isopropoxide precursor.

| Ti (%) | BET SA (m ² .g ⁻¹) |
|--------|---|
| 0 | 920 |
| 10 | 670 |
| 15 | 547 |

F. Characterizations of the samples obtained *in-situ* using TiBALD.

Table S6: EDS data for samples obtained using TiBALD precursor (9 points analysis).

| SAMPLE | THEOR Ti/Zr | AVERAGE Ti/Zr | STANDARD DEVIATION |
|--------|-------------|---------------|--------------------|
| 5% Ti | 0.05 | 0.048 | 0.007 |
| 10% Ti | 0.11 | 0.10 | 0.01 |
| 30% Ti | 0.43 | 0.41 | 0.02 |
| 40% Ti | 0.67 | 0.71 | 0.05 |
| 50% Ti | 1 | 1.1 | 0.05 |

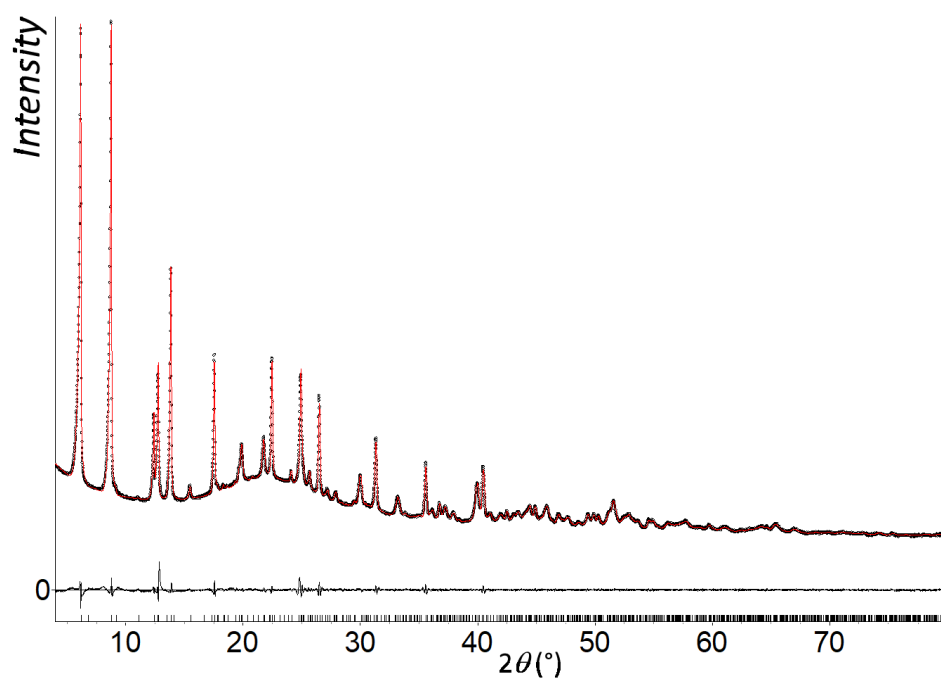


Figure S6: Whole powder pattern decomposition of MIL-173(Zr).

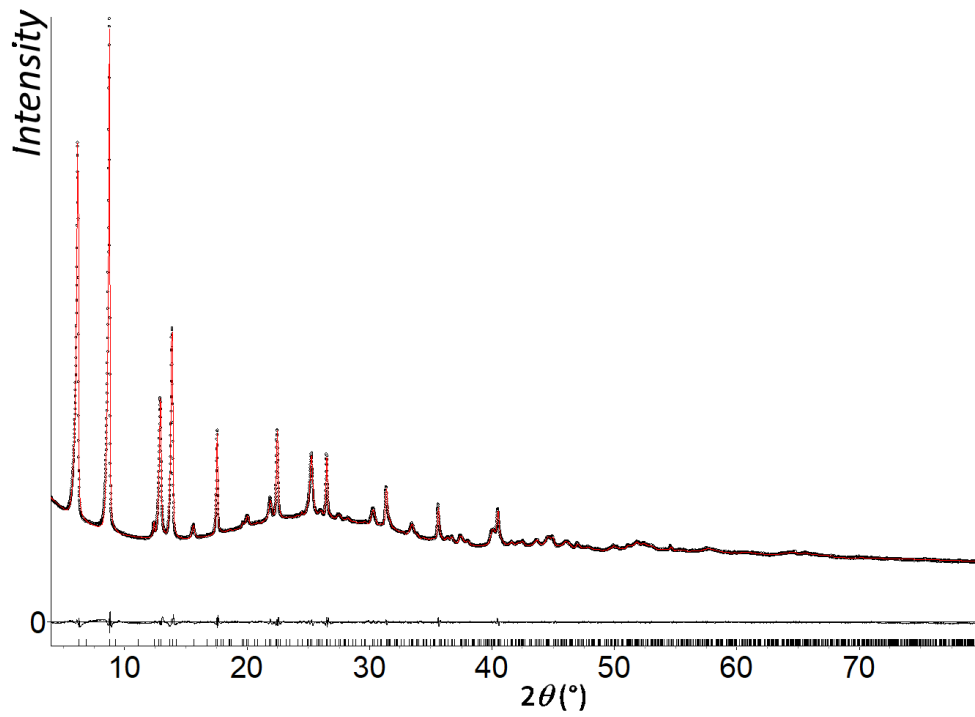


Figure S7: Whole powder pattern decomposition of 10% at Ti containing MIL-173(Ti/Zr)-10.

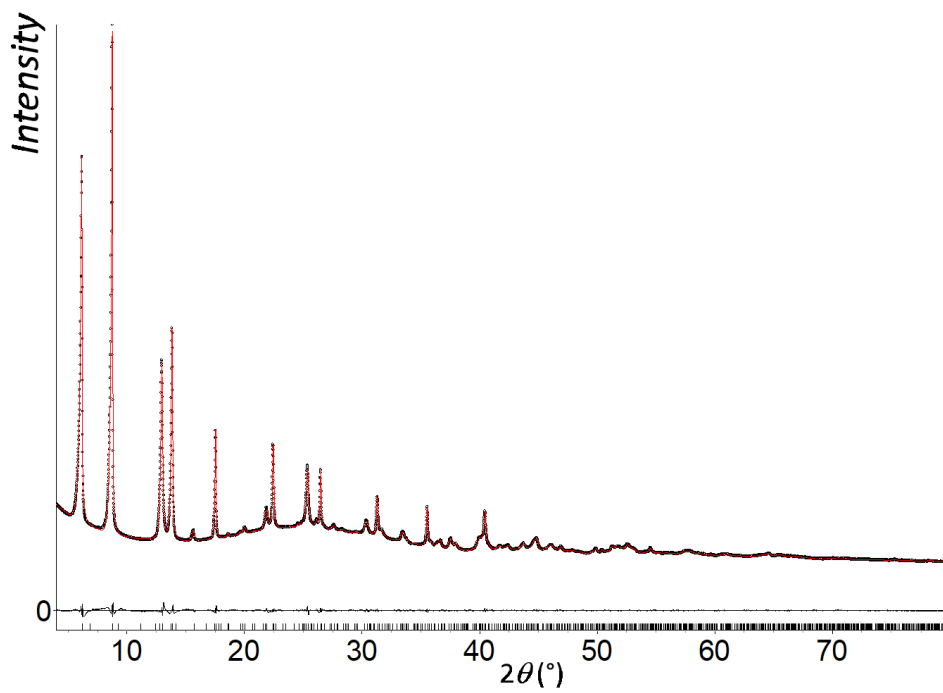


Figure S8: Whole powder pattern decomposition of 20% at Ti containing MIL-173(Ti/Zr)-20.

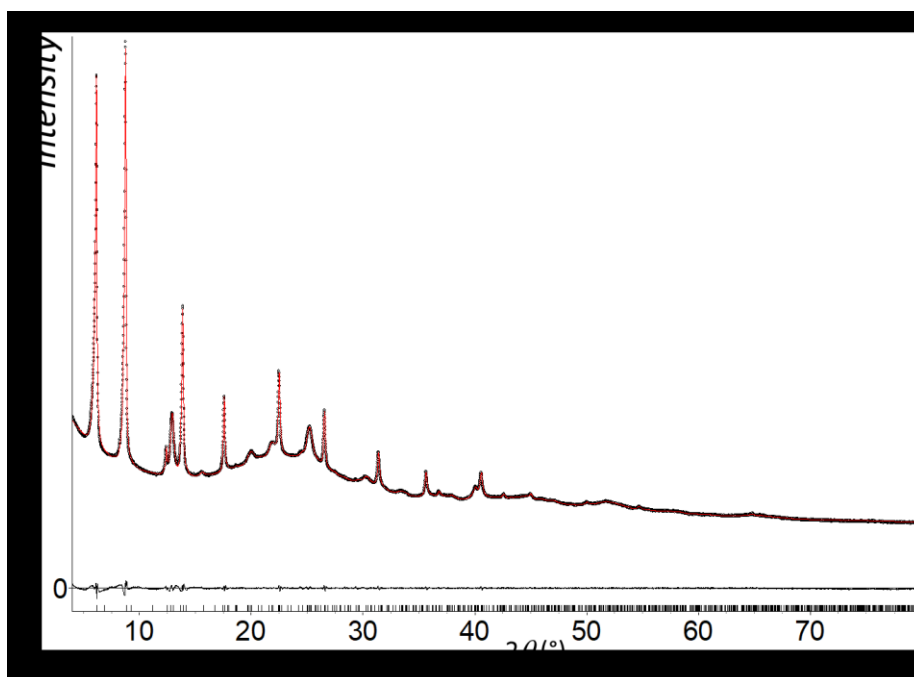


Figure S9: Whole powder pattern decomposition of 35% at Ti containing MIL-173(Ti/Zr)-35.

Table S7: Cell parameters from pattern matching.

| Ti at% | a (Å) | c (Å) | V (Å ³) |
|--------|------------|------------|-----------------------|
| 0 | 28.4906(4) | 14.7290(5) | 11955.7(5) |
| 10 | 28.4735(4) | 14.5156(4) | 11768.4(5) |
| 20 | 28.5167(3) | 14.4558(3) | 11755.5(3) |
| 35 | 28.4346(5) | 14.482(2) | 11708(2) |

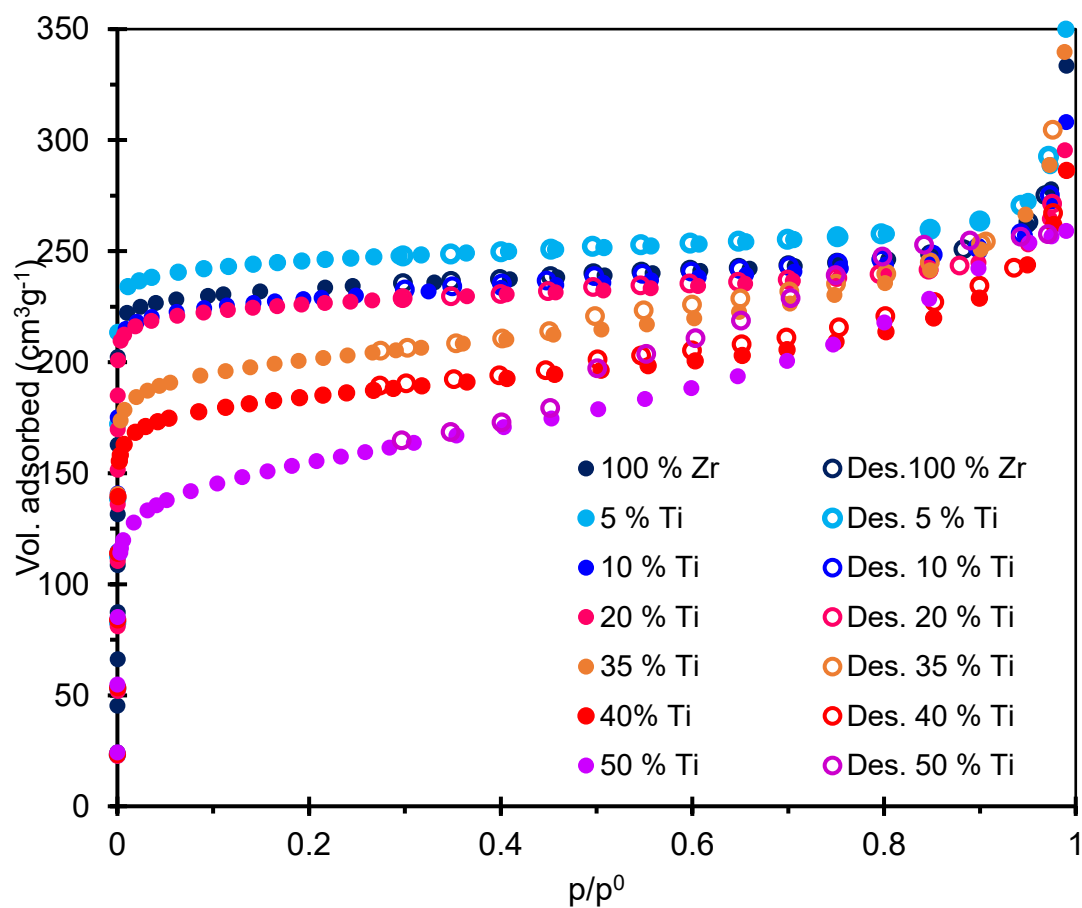


Figure S10: Nitrogen sorption isotherms at 77K for samples synthesized in-situ using TiBALD precursor

Table S8: BET surface area for samples synthesized in-situ using TiBALD precursor

| Ti (%) | BET SA (m ² .g ⁻¹) |
|--------|---|
| 0 | 920 |
| 5 | 960 |
| 20 | 900 |
| 35 | 780 |
| 40 | 715 |
| 50 | 570 |

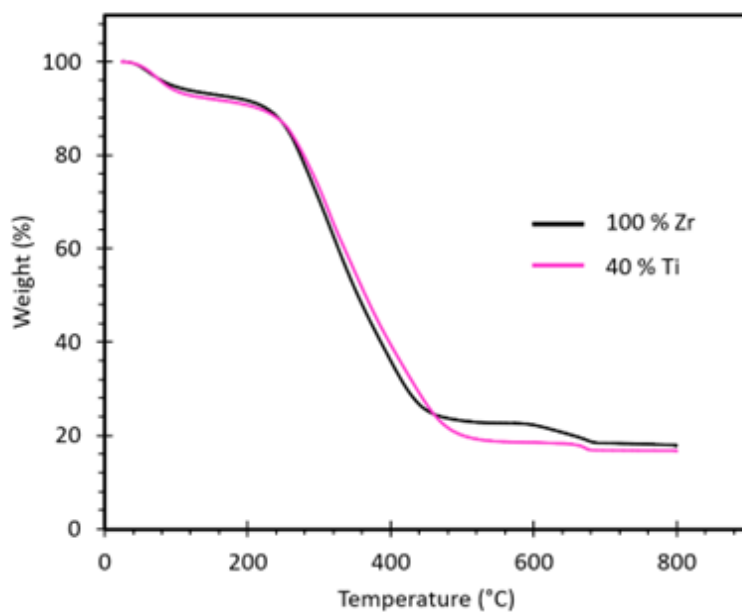


Figure S11: TGA data for the MIL-173(Zr) and MIL-173(Zr/Ti)-40 under air, heating at 10°C/min

Table S9: Weight percentage of oxide obtained for MIL-173(Zr), and MIL-173(Ti/Zr)-40 samples synthesized in-situ using TIBALD precursor.

| sample | % wt. oxide calculated | % wt. oxide experimental |
|----------|------------------------|--------------------------|
| 100 % Zr | 19.1 % | 18 % |
| 40 % Ti | 16.98 % | 16.8 % |

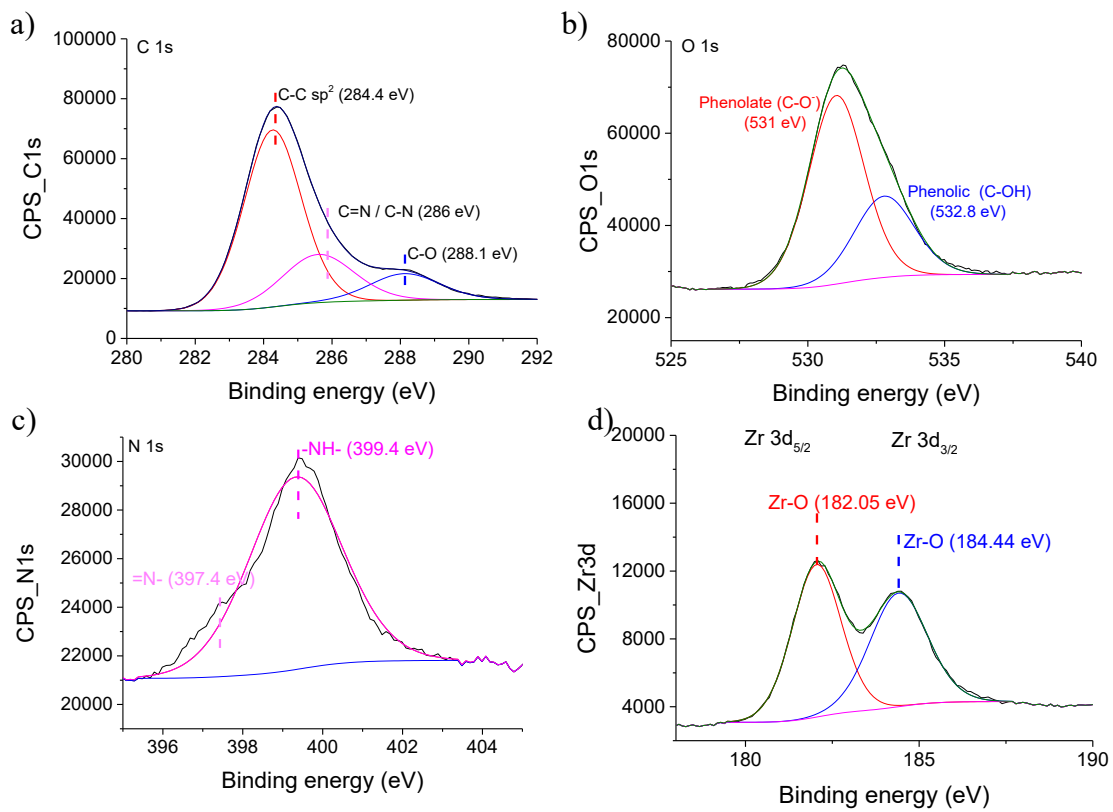


Figure S12: XPS C 1s (a), O 1s (b), N 1s (c) and Zr 3d (d) of the MIL-173(Zr) sample.

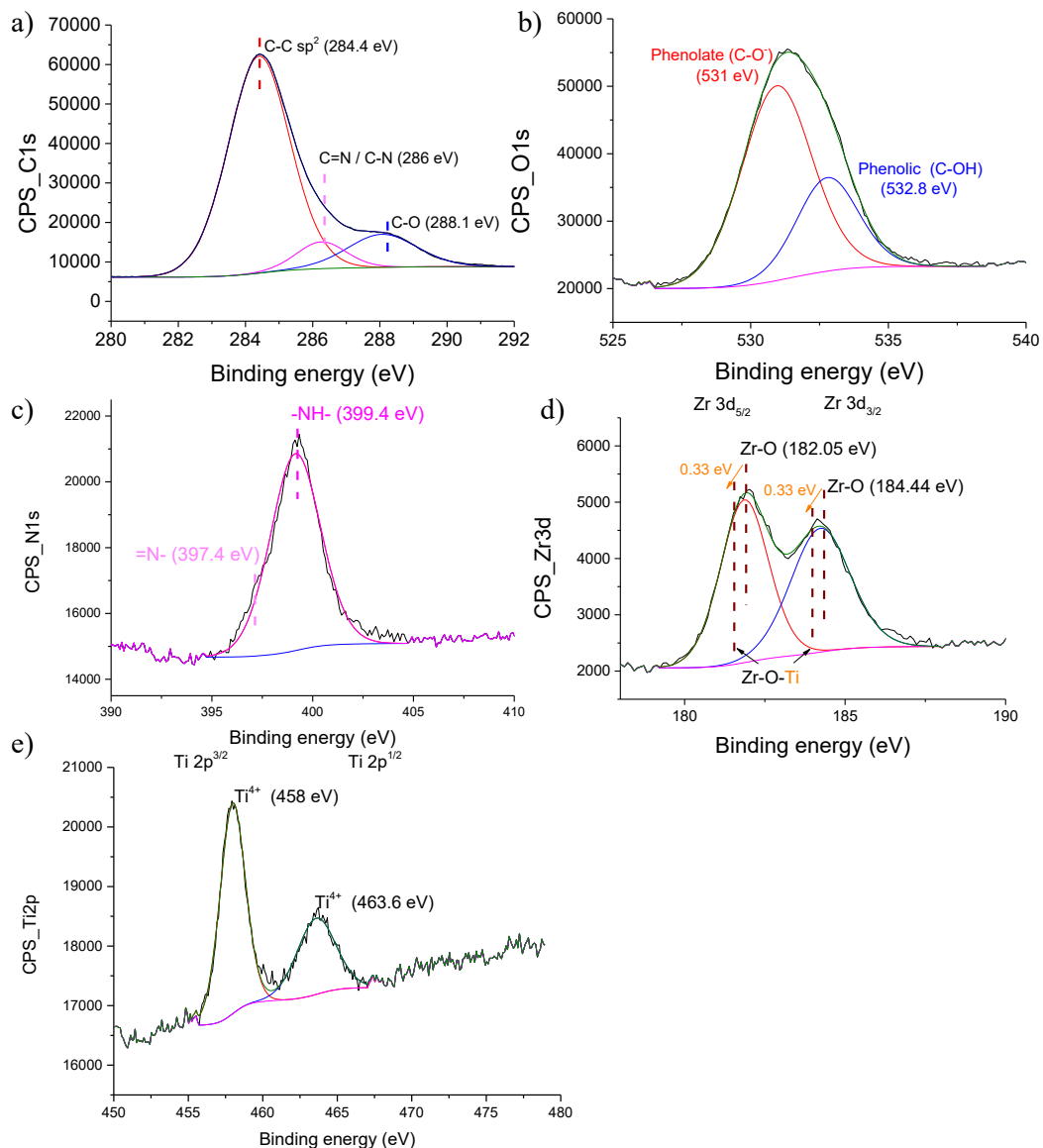


Figure S13: XPS C 1s (a), O 1s (b), N 1s (c), Zr 3d (d) and Ti 2p of the MIL-173(Zr/Ti)-40 sample.

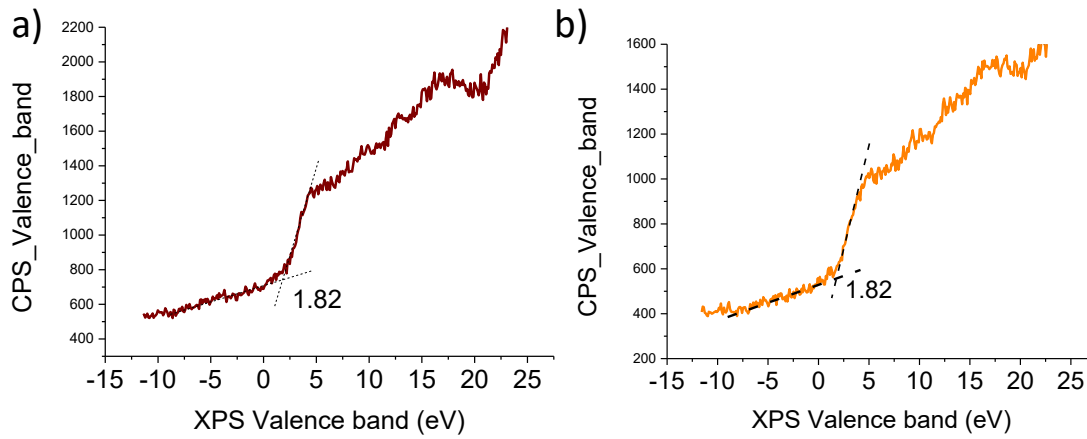


Figure S14: XPS valence bands for MIL-173(Zr) (a) and MIL-173(Zr/Ti)-40 (b) samples.

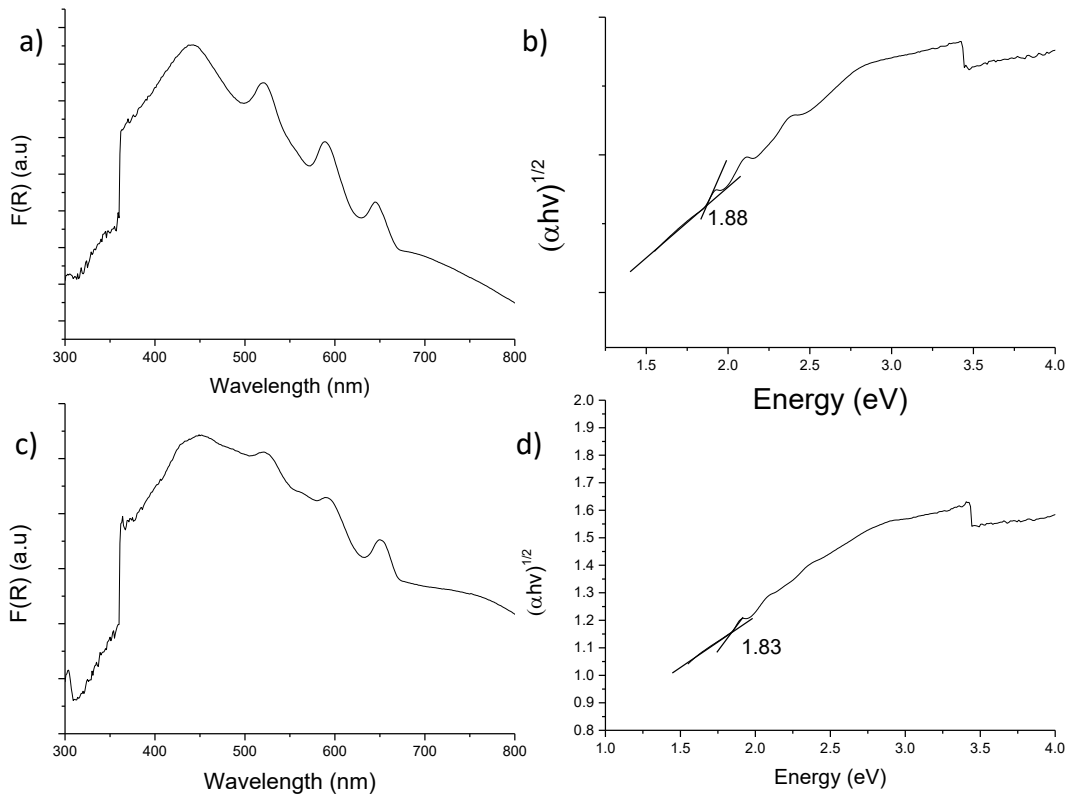


Figure S15: UV-vis diffuse reflectance (a, c) and Tauc plots (b, d) for MIL-173(Zr) (a, b) and MIL-173(Zr/Ti)-40 (c, d)

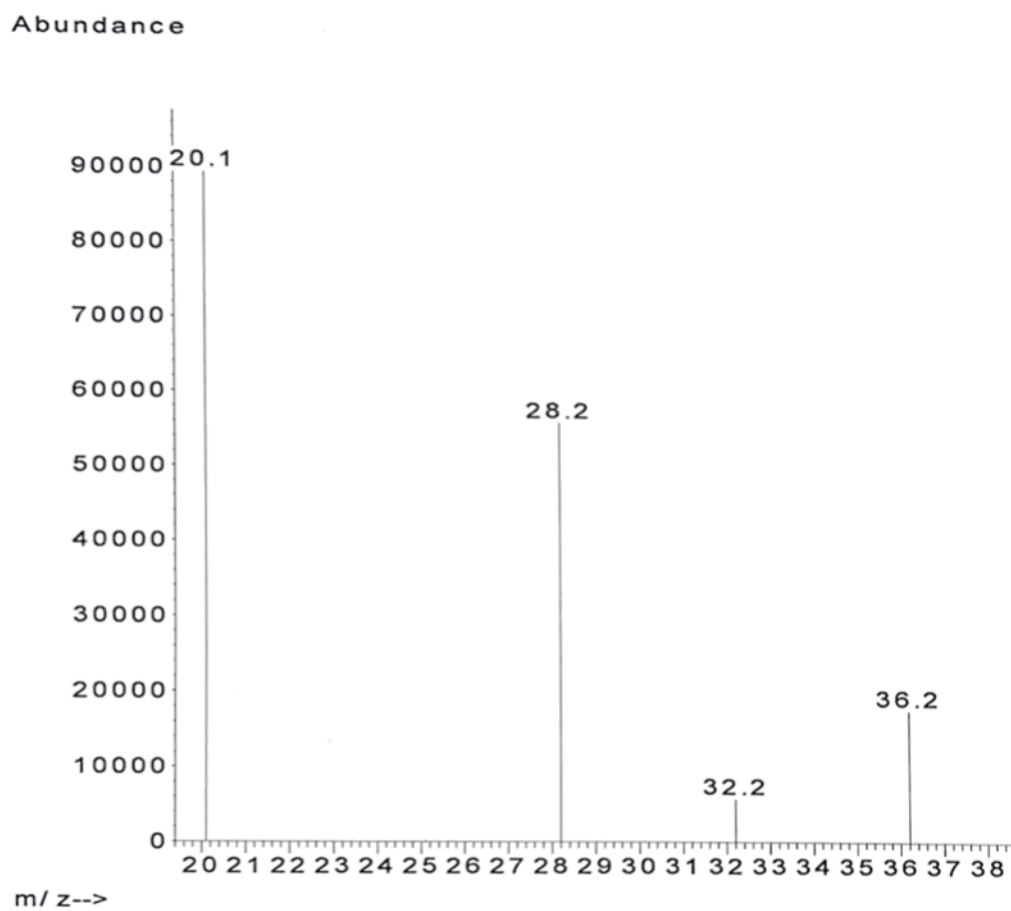


Figure S16: Mass spectrum obtained from headspace gas during the photocatalytic OWS under simulated sunlight irradiation in the presence of MIL-173(Zr/Ti)-40 solid dispersed in labelled $H_2^{18}O$ as reaction medium. Reaction conditions: photocatalyst (2 mg), $H_2^{18}O$ (4 mL), simulated sunlight (Hg-Xe lamp 150 W equipped with an AM 1.5G filter), 35 °C, reaction time 22 h

G. Characterizations of the samples after photocatalysis

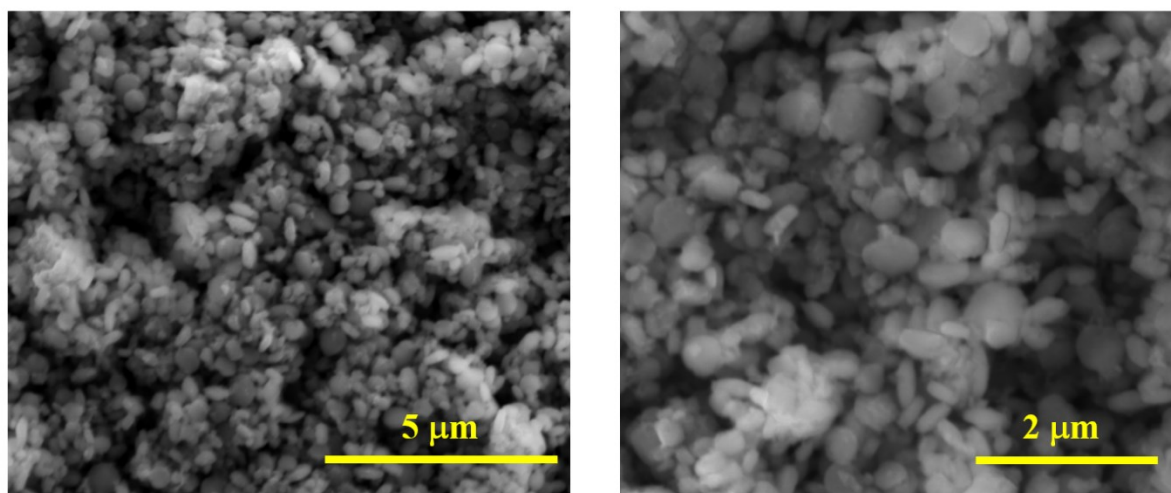


Figure S17: SEM images of MIL-173(Zr/Ti)-40 after 3 photocatalytic cycles.

Table S10: The EDS data from 9 points analysis of MIL-173(Zr/Ti)-40 after 3 photocatalytic cycles.

| Theoretical Ti/Zr | AVERAGE Ti/Zr | STANDARD DEVIATION |
|-------------------|---------------|--------------------|
| 0.67 | 0.62 | 0.08 |

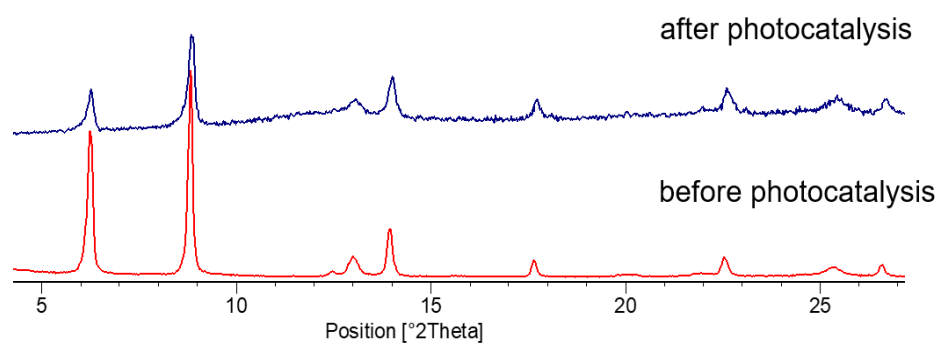


Figure S18: PXRD patterns of MIL-173(Zr/Ti)-40 before and after 3 cycles of photocatalytic OWS.

References

- 1 L. Jiang, F. Lu, H. Li, Q. Chang, Y. Li, H. Liu, S. Wang, Y. Song, G. Cui, N. Wang, X. He and D. Zhu, *J. Phys. Chem. B*, 2005, **109**, 6311–6315.
- 2 Y.-G. Yu, G. Chen, L.-X. Hao, Y.-S. Zhou, Y. Wang, J. Pei, J.-X. Sun and Z.-H. Han, *Chem Commun*, 2013, **49**, 10142–10144.
- 3 P. Giannozzi, S. Baroni, N. Bonini, M. Calandra, R. Car, C. Cavazzoni, D. Ceresoli, G. Chiarotti, M. Cococcioni, I. Dabo, A. Dal Corso, S. de Gironcoli, S. Fabris, G. Fratesi, R. Gebauer, U. Gerstmann, C. Gougoussis, A. Kokalj, M. Lazzeri, L. Martin-Samos, N. Marzari, F. Mauri, R. Mazzarello, S. Paolini, A. Pasquarello, L. Paulatto, C. Sbraccia, S. Scandolo, G. Sclauzero, A. Seitsonen, A. Smogunov, P. Umari and R. Wentzcovitch, *J. Phys.-Condens. MATTER*, , DOI:10.1088/0953-8984/21/39/395502.
- 4 J. P. Perdew, A. Ruzsinszky, G. I. Csonka, O. A. Vydrov, G. E. Scuseria, L. A. Constantin, X. Zhou and K. Burke, *Phys Rev Lett*, 2008, **100**, 136406.
- 5 J.-W. Song, K. Yamashita and K. Hirao, *J. Chem. Phys.*, 2011, **135**, 071103.
- 6 D. Ongari, P. G. Boyd, S. Barthel, M. Witman, M. Haranczyk and B. Smit, *Langmuir*, 2017, **33**, 14529–14538.
- 7 T. F. Willems, C. H. Rycroft, M. Kazi, J. C. Meza and M. Haranczyk, *Microporous Mesoporous Mater.*, 2012, **149**, 134–141.
- 8 G. Mouchaham, B. Abeykoon, M. Giménez-Marqués, S. Navalon, A. Santiago-Portillo, M. Affram, N. Guillou, C. Martineau, H. Garcia, A. Fateeva and T. Devic, *Chem. Commun.*, 2017, **53**, 7661–7664.